

Efficient Heating at the Third Harmonic Electron Cyclotron Resonance in Large Helical Device

Takashi SHIMOZUMA¹⁾, Shin KUBO¹⁾, Hiroe IGAMI¹⁾, Yasuo YOSHIMURA¹⁾, Takashi NOTAKE²⁾, Nikolai B. MARUSHCHENKO³⁾, Yuriy. TURKIN³⁾, Takashi MUTOH¹⁾ and LHD Experimental Group¹⁾

¹⁾National Institute for Fusion Science, 322-6 Oroshi-cho, Toki 509-5292 Japan

²⁾University of Fukui, Research Center for Development of Far-Infrared Region, 3-9-1 Bunkyo, Fukui 910-8507 Japan

³⁾Max-Planck-Institut für Plasmaphysik, EURATOM-Association, Greifswald, Germany

(Received / Accepted)

Efficient heating at the third harmonic electron cyclotron resonance was attained by injection of millimeter-wave power with 84 GHz frequency range at the magnetic field strength of 1 T in LHD. The plasma center clearly increased and the increment of the temperature reached 0.2 – 0.3 keV. Dependence of the power absorption rate on the antenna focal position was experimentally investigated, showing that the optimum position located in the slightly high-field side of the resonance layer. Ray-tracing calculation was performed in the realistic three-dimensional magnetic configuration. The results are compared with the experimental results.

Keywords: electron cyclotron resonance heating, gyrotron, harmonic resonance, quasi optical antenna, ray tracing

DOI: 10.1585/pfr.1.001

1. Introduction

High harmonic heating of the electron cyclotron resonance (ECR) is an attractive method to extend a heating regime of plasma parameters by alleviating the density limitation due to some cutoffs of the EC wave propagation. In the LHD launching geometry, the magnetic field strength is almost constant along the ray paths launched from upper- and lower-port antennas which cross near the magnetic axis. Under this condition, the ray can keep resonant with the plasma over a considerable length. So good absorption is predicted over a wide density range even for the 3rd harmonic heating by the linear theory [1].

Experimentally the 3rd harmonic heating was tried in Heliotron DR and effective heating was observed [2]. In TCV tokamak, 3rd harmonic heating was carried out with the 2nd harmonic heating by using two different frequency gyrotrons such as 82.7 GHz for the 2nd harmonic and 118 GHz for the 3rd harmonic resonance. Hundred percent absorption was attained on existence of high energy electrons produced by the 2nd harmonic resonance heating [3, 4]. After that, the sophisticated feedback control of antenna focal position realized 100 % absorption by only 3rd harmonic resonance heating [5]. In W7-X, the 3rd harmonic heating is planned as a candidate of a normal heating scenario in the high density regime ($0.6 - 2.0 \times 10^{20} \text{ m}^{-3}$) by using 140 GHz, 10 MW ECH system [6].

Effective 3rd harmonic heating has been already achieved on the 2 T LHD plasma by injection of 168 GHz millimeter wave power from upper-port antennas. In the

experiments of the 3rd harmonic resonance heating, obvious heating of the bulk plasma ($\Delta T_e = 0.2 \text{ keV}$) around the plasma center by 340 kW power injection was observed [7].

Because ECH power of 84 GHz range has been upgraded up to 1.3 MW recently, we have tried the 3rd harmonic extraordinary(X)-mode heating by injection of 84 GHz range power at the magnetic field strength of 1 T with the magnetic axis of 3.75 m. When the same frequency is used, a cutoff density for the 3rd harmonic X-mode heating at 1 T becomes 4/3 higher than that for 2nd harmonic X-mode heating at 1.5 T. It is about $6 \times 10^{19} \text{ m}^{-3}$.

2. Experimental setup and results

The ECH system consists of 84 GHz range and 168 GHz gyrotrons, high voltage power supplies, long distance transmission lines, and in-vessel quasi-optical antennas. It has been improved step by step. At the last campaign(2006) of LHD experiments five 84 GHz range and three 168 GHz gyrotrons are operated and ECH power could be injected from six antennas in the vertically elongated cross section (upper-port and lower-port antennas) and two antennas in the horizontally elongated cross section(outer-port antennas).

Two kinds of antenna systems for ECH are installed in the LHD vacuum vessel. The vertical injection antenna system consists of four or two millimeter-wave focusing and steering mirrors. High power measurement of this system shows a good agreement with the designed beam-waist size of 15 mm in radial and 50 mm in toroidal direction for the upper-port antennas and of 30 mm for the lower-port

antennas. The direction of the beam can be steered radially and toroidally. The injected millimeter-wave beams from these antennas consequently have a grazing incidence angle to the cyclotron resonance and continues to interact along a long ray-path. For horizontal injection, the antenna system consists of 2 mirrors, one is fixed and another is steerable. Movable range covers the whole plasma cross section for perpendicular injection and can change about ± 30 degrees toroidally. In this case, the injected beams perpendicularly pass through the ECR layer with the shortest gradient length.

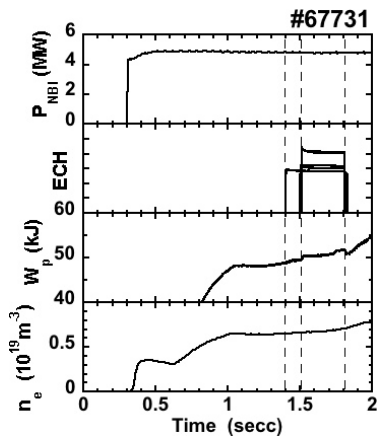


Fig. 1 Wave form of NBI power, ECH timing, stored energy W_p and line-averaged density from top to bottom.

A magnetic configuration was chosen such that the 3rd harmonic electron cyclotron resonance located on the magnetic axis for both in the vertically and horizontally elongated cross sections, because microwave beams from all antennas could access almost perpendicularly to the magnetic field line of force. So the magnetic field strength of 1 T on the magnetic axis placed on $R_{ax} = 3.75$ m was adopted.

In the experiments, target plasmas were produced and sustained by only NBI power. The electron temperature of a target plasma was about 1 keV and the line-averaged density was $0.6 \times 10^{19} \text{m}^{-3}$ at the center. ECH power (1.3 MW) was injected from $t=1.4$ sec and 1.5 sec stair-likely as shown in Fig. 1. The ECH pulse which has a longer pulse width corresponds to 84 GHz power from the outer-port antenna. The ECH pulse with a shorter pulse width is 82.7 GHz from top-antennas and 84 GHz from bottom-antennas. The absorption rate for the different way of resonance can be discriminated independently and effectively by the stair-like injection. Obvious increase of the stored energy was observed during both the first and second ECH pulses, while there was no change in the density.

Figure 2 shows electron temperature profiles just before ($t=1.37$ sec) and during ($t=1.57$ sec) ECH power injection. The plasma center was efficiently heated, and the

increment of the temperature reached 0.2 – 0.3 keV.

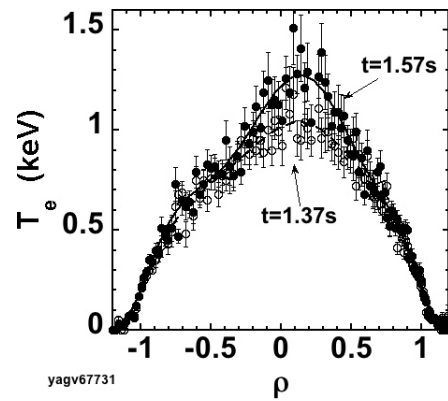


Fig. 2 Electron temperature profiles just before ($t=1.37$ sec) and during ($t=1.57$ sec) ECH. ρ is the normalized minor radius.

Absorbed power was estimated by the increment of the plasma stored energy dW_p/dt before and after ECH on-timing, assuming that the other plasma parameters did not change so much. The dependence on the focal point R_{foc} of the upper-port antennas (82.7 GHz) was examined in special(Fig. 3). The maximum absorption rate was obtained on the antenna focal position $R_{foc}=3.7$ m, which was slightly smaller than the 3rd harmonic ECR layer (3.75m). The absorption rate, however, is rather low, because the temperature and density of the target plasma was fairly low. The absorption rate for the other antennas were estimated to be about 8 %.

Detailed calculations by ray-tracing in the LHD magnetic configuration is required to discuss the absorption rate and its dependence on the antenna focal point.

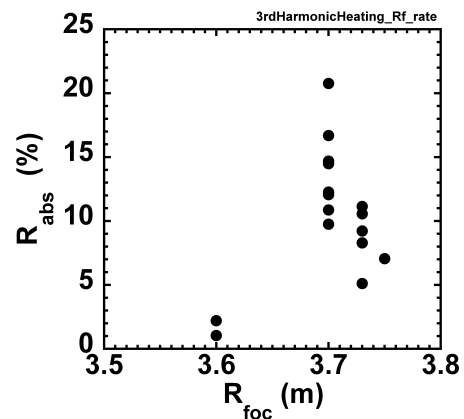


Fig. 3 Efficiency of absorbed power for 82.7GHz antenna was estimated by change of dW_p/dt at ECH on-timing. Antenna focal point on the equatorial plane R_{foc} dependence is shown.

3. Preliminary ray-trace calculation in LHD magnetic configuration

In order to estimate the absorption rate, ray trace calculation was carried out for a given electron temperature and density profiles in the LHD magnetic field configuration.

The ray-tracing code, "TRAVIS (IPP)", has been developed for ECH/ECCD and ECE studies in an arbitrary three-dimensional magnetic configuration [8, 9]. The basic ray-tracing equations include weakly relativistic formulation for Hamiltonian with taking into account possible anomalous dispersion effects. Gaussian power distribution of an injected beam is assumed and the beam cross-section is discretized by the arbitrary number of radial and azimuthal points. The wave absorption can be calculated in fully relativistic formulation. The power deposition is decomposed for passing and trapped electrons contributions.

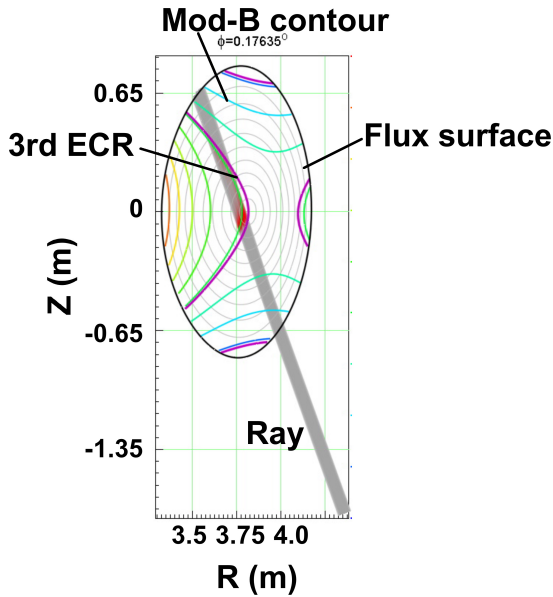


Fig. 4 Ray trace calculation together with mod-B contours and flux surfaces.

An X-mode is assumed to be perpendicularly injected from the lower-port antenna focused on the magnetic axis. In Fig. 4, the configuration of calculation is illustrated with mod-B counters, flux surfaces and wave rays. The 3rd harmonic electron cyclotron resonance is also depicted. Calculated rays from the lower-port antenna are typically shown. The profile of the electron temperature is assumed $(T_{e0} - T_{ea}) \times (1 - \rho^3)^{1.5} + T_{ea}$ with $T_{e0}=1.3$ keV, where $\rho = r/a$ is a normalized minor radius, and T_{e0} and T_{ea} are the electron temperature at the plasma center and the edge, respectively. The central electron density n_{e0} is assumed to be $1 \times 10^{19} \text{m}^{-3}$. The profile of the electron density was assumed the same as the electron temperature.

The power absorption is localized near the 3rd harmonic resonance ($B = 1$ T) and the deposition is almost limited within $\rho \sim 0.2$, which is shown in Fig. 5 (a). Most

part of the power is absorbed by the passing electrons near the magnetic axis. A small fraction is absorbed by the trapped electrons within $\rho \sim 0.2$ and around $\rho \sim 0.4 - 0.5$. The integrated absorbed power is shown in Fig. 5 (b). Total amount of the absorption power reaches 0.6 MW for 1.3 MW injection. Maximum absorption rate is about 50 %.

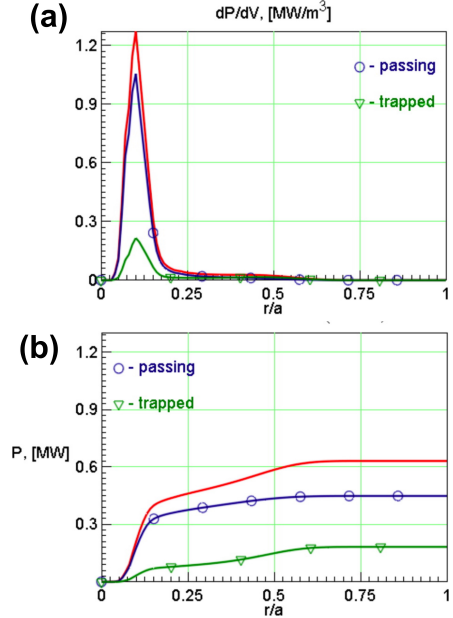


Fig. 5 Power deposition. (a) Deposited power density is plotted as a function of normalized minor radius and (b) integral value of absorbed power along the ray path. Total amount is decomposed into each component absorbed by passing and trapped electrons.

4. Discussion and summary

The experimental results show the efficient heating at the 3rd harmonic resonance even in the fairly low electron temperature (~ 1 keV) and low electron density ($\sim 0.6 \times 10^{19} \text{m}^{-3}$). However experimentally obtained absorption rate of about 20 % is lower than that expected by the ray-tracing calculation, which was carried out in the realistic three-dimensional magnetic configuration of LHD. One possible reason of the discrepancy seems to be the differences of values and profiles of the temperature and density for between the actual plasma and the modeled one. Because the optical thickness scales as $\tau \sim n_e \cdot T_e^2$, a little temperature change possibly leads to fairly large difference of the absorption rate. Figure 6 shows a contour-plot of the single-pass absorption rate in the electron temperature and density space for the injection from the upper-port antenna with $R_{foc} = 3.7$ m. In these calculations the dispersion relation of a cold plasma was assumed for ray calculation and the weakly relativistic effect were included for the absorption [10]. The profiles of the electron temperature and density are assumed to have the same ones such as $(1 - \rho^2)^2$.

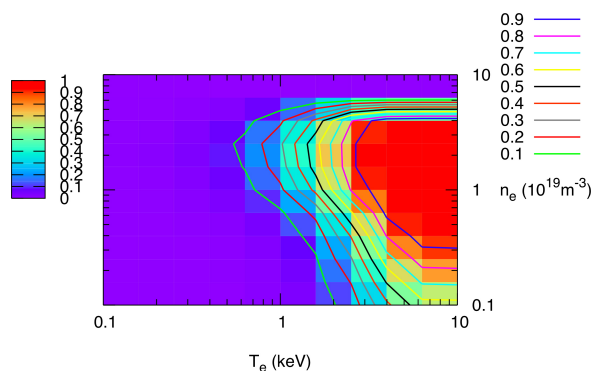


Fig. 6 Single-pass absorption rate for the injection from upper-port antenna is contour-plotted in the electron temperature and density space.

The values of temperature, T_e , and density, n_e , in the figure represent the values in the center. The figure clearly shows almost 100 % absorption is expected in the high temperature (≥ 3 keV) and high density ($1 - 4 \times 10^{19} \text{m}^{-3}$) region up to the right-hand cut-off density. However in the low temperature (≤ 1 keV) and low density ($\leq 1 \times 10^{19} \text{m}^{-3}$), the absorption rate can change from several percent to several tens percent according to the small change of plasma parameters.

Another possible reason is the production of supra-thermal electrons by the 3rd harmonic ECR, which could be drifting out from a plasma quickly before thermalization and do not contribute to the increment of diamagnetic energy of the plasma. These facts can partly explain the discrepancy between the values of the single-pass absorption calculated by the ray-tracing and the absorption rate evaluated from the temporal change of dW_p/dt .

In summary, the 3rd harmonic electron cyclotron resonance heating experiments were performed. Especially, because of the upgrade of 84 GHz gyrotrons and transmission line, the efficient heating results were obtained even for the 3rd harmonic resonance. During the ECH pulse of 0.4 sec. stored energy of the plasma increased several percents. The central electron temperature raised about 0.2 – 0.3 keV. Dependence of the absorption rate on the antenna focal position shows the maximum at a slightly higher-field side of the resonance position. Preliminary calculation using ray-tracing code "TRAVIS", which has been developed in IPP Greifswald (Germany), was successfully carried out in the three-dimensional magnetic configuration of LHD.

In order to discuss a detailed quantitative comparison is required between experimental and calculated results for the optimization of the heating efficiency in view of injection configuration. These works are under way.

Acknowledgment

The authors gratefully acknowledge the LHD technical group for their sophisticated operation of LHD, and the

heating and diagnostic devices. They also thank Professors A. Komori, S. Sudo and O. Motojima for their continuous guidance and encouragement. This work has been supported by NIFS under NIFS06ULRR501,502,503.

- [1] U. Gasparino, H. Idei, S. Kubo, et al., Nuclear Fusion, 38(1998)pp223-235.
- [2] N. Yanagi, S. Morimoto, M. Sato et al., Nuclear Fusion, 31(1991)261-271.
- [3] S. Alberti, T. P. Goodman, M.A. Henderson, et al., Nuclear Fusion 42(2002)pp42-45
- [4] G. Arnoux et al, Plasma Phys. Control. Fusion 47(2005)295-314
- [5] S. Alberti et al, Nucl. Fusion 45(2005)1224-1231
- [6] H. P. Laqua, V. Erckmann, R. Brakel, et al., 15th International Stellarator Workshop, Madrid,3-7, October 2005, IT-20.
- [7] T. Shimozuma, H. Idei, et al., 27th European Physical Society Conference on Controlled Fusion and Plasma Physics, Budapest, Hungary, June 12-16, 2000, P4.019
- [8] N. B. Marushchenko, V. Erckmann, H. Maaßberg, Yu. Turkin, 34th European Physical Society Conference on Plasma Physics, Warsaw, Poland, July 2-6, 2007, P5.129.
- [9] N. B. Marushchenko et al., to be published in Plasma and Fusion Research, 2007.
- [10] S. Kubo, T. Shimozuma et al., Plasma Phys. Control. Fusion 47(2005)A81-A90.